Distributed Joint Source-Channel Coding with Copula-Function-Based Correlation Modeling for Wireless Sensors Measuring Temperature

Nikos Deligiannis, Evangelos Zimos, Dragos Mihai Ofrim, Yiannis Andreopoulos, and Adrian Munteanu

Abstract—Wireless sensor networks (WSNs) deployed for temperature monitoring in indoor environments call for systems that perform efficient compression and reliable transmission of the measurements. This is known to be a challenging problem in such deployments, as highly-efficient compression mechanisms impose a high computational cost at the encoder. In this paper, we propose a new distributed joint source-channel coding (DJSCC) solution for this problem. Our design allows for efficient compression and error-resilient transmission, with low computational complexity at the sensor. A new Slepian-Wolf code construction, based on non-systematic Raptor codes, is devised that achieves good performance at short code lengths, which are appropriate for temperature monitoring applications. A key contribution of the work is a novel Copula-function-based modeling approach that accurately expresses the correlation amongst the temperature readings from co-located sensors. Experimental results using a WSN deployment reveal that, for lossless compression, the proposed Copula-function-based model leads to a notable encoding rate reduction (of up to 17.56%) compared to the state-of-the-art model in the literature. Using the proposed model, our DJSCC system achieves significant rate savings (up to 41.81%) against a baseline system that performs arithmetic entropy encoding of the measurements. Moreover, under channel losses, the transmission rate reduction against the state-of-the-art model reaches 19.64%, which leads to energy savings between 18.68% to 24.36% with respect to the baseline system.

Index Terms—Wireless sensor networks (WSNs), Distributed joint source-channel coding (DJSCC), Correlation Modeling, Copula function, Temperature monitoring.

I. INTRODUCTION

WIRELESS sensor networks (WSNs) operate under austere constraints in terms of energy resources, computational capabilities and available bandwidth [1]. Many WSN applications (e.g., temperature or humidity monitoring, wireless visual sensors) involve a high density of sensors within an environment, thereby sensors' readings are highly correlated. In order to minimize the amount of information transmitted by the sensors, this redundancy needs to be removed by efficient data compression mechanisms that have low computational

N. Deligiannis and Y. Andreopoulos are with the Electronic and Electrical Engineering Department, University College London, Roberts Building, Torrington Place, London, WC1E 7JE, UK. (email: n.deligiannis@ucl.ac.uk; i.andreopoulos@ucl.ac.uk).

Dragos Mihai Ofrim is with InterNET SRL, OFRIM Group Member, Piata Lahovari Street, fl. 4, ap. 10, district 1 RO 010464, Bucharest, Romania (e-mail: dragos.ofrim@ofrimgroup.com).

E. Zimos and A. Munteanu are with the Department of Electronics and Informatics, Vrije Universiteit Brussel, Pleinlaan 2, 1050 Brussels, Belgium, and with iMinds, Gaston Crommenlaan 8 (b102), 9050 Ghent, Belgium (email: ezimos@etro.vub.ac.be; acmuntea@etro.vub.ac.be).

demands. In addition, as information is sent over error-prone wireless channels, effective data protection mechanisms are required to provide for reliable communications.

In this setting, distributed source coding (DSC) is considered a key technology for WSNs [2]. DSC is rooted in the information-theoretic results by Slepian and Wolf [3]—on lossless compression of correlated sources—and by Wyner and Ziv [4]—on lossy compression with side information at the decoder. The multiterminal (MT) source coding theory [5] extended these results to an arbitrary number of correlated sources [6]. DSC designs [2], [7], [8] exploit the correlation amongst the sensors' readings at the decoder, i.e., the base station or sink node. In this way, efficient compression is obtained by shifting the complexity to energy-robust nodes and keeping the sensor computational and energy demands to a minimum. In addition, energy expensive data exchange between sensors is avoided. Moreover, as Slepian-Wolf coding is realized by channel codes (e.g., Turbo [9], low-density parity-check [10] or Raptor [11] codes), distributed joint source-channel coding (DJSCC) [12] designs offer resilience against communication channel errors [12]. Hence, it is recognized [2], [13], [14] that, in correlated data gathering by energy-constrained WSNs, DSC schemes have distinct advantages over predictive coding systems that apply complex adaptive prediction and entropy coding at the encoder.

A. Related Work

Several works have studied DSC for wireless sensors monitoring temperature. Towards practical schemes, a construction realizing Slepian-Wolf (SW) coding for two sensors measuring the temperature in a room was devised in [16]. In the latter, SW coding was realized by means of a simple coset construction. In order to exploit the spatial correlations in time-varying environments, rate adaptation was enabled based on an entropy tracking algorithm. The construction of [16] was extended to a cross-layer design by modeling the interaction between DSC and the medium access control (MAC) layer [17].

Concerning lossy distributed compression, a Wyner-Ziv code design comprising quantization followed by binarization and LDPC encoding was proposed in [18]. Considering a multi-sensory scenario, the author of [19] introduced a MT code design in which SW coding was simply replaced by entropy coding, whereas joint source reconstruction at the decoder was realized by Gaussian process regression.

Temperature readings from sensors are typically modeled as jointly Gaussian, namely, the spatial correlation is character-

ized by a multivariate Gaussian distribution [16], [18], [19]. This assumption is also typically encountered in information-theoretic studies [13], code designs [20] and correlation estimation works [21]. Alternatively, the authors of [22] studied MT source coding under physical models of heat diffusion. In particular, they focused on heat conduction in solid bodies (rail temperature monitoring applications) and derived upper and lower bounds on the rate-distortion performance.

B. Contributions

This paper proposes a novel DJSCC design for WSNs measuring temperature. Our specific contributions are:

- We propose a novel modeling approach for the spatial correlation of the sensors' measurements. Contrary to the multivariate Gaussian model, typically considered in state-of-the-art works [13], [18], [19], [21], the proposed approach models the marginal distributions of the data using density kernel estimation and expresses the correlation using a Copula function [23], [24]. In this way, the proposed approach offers a higher modeling accuracy than the conventional multivariate Gaussian model, leading to significant coding improvements.

- Existing coding schemes for temperature data collected by sensors, e.g., [15], [18], [19], [25]–[27], focus only on data compression. On the contrary, the proposed DJSCC design *jointly* addresses compression and error-resilient transmission of data. In this way, channel impairments are mitigated without requiring packet retransmissions at the MAC layer, thereby leading to significant energy savings for each sensor.

- We devise a novel scheme using asymmetric SW coding realized by Raptor codes [28], the newest class of rateless channel codes—implementations of which have already been proposed for embedded systems [29]. Our code design is specifically tailored to the requirements of temperature monitoring by WSNs: Conversely to existing designs that focus on video coding [12] or consider generic binary sources [11], our SW code construction is based on non-systematic Raptor codes that achieve good performance for short code lengths.

- Experimental results using real data from a proprietary WSN deployment show that the proposed system introduces significant compression gains (up to 41.81% in rate reduction) with respect to the baseline scheme that performs arithmetic entropy coding of the data. In addition, the proposed Copula-function-based model is shown to lead to a significantly higher source and channel coding performance compared to the state-of-the-art multivariate Gaussian model.

- Finally, via our WSN deployment, we show that the proposed system results in systematic and notable energy savings at the sensor nodes, between 18.68% to 24.36% with respect to the baseline system.

C. Outline

Section II describes the considered WSN model and gives an introduction to SW coding. The proposed DJSCC architecture
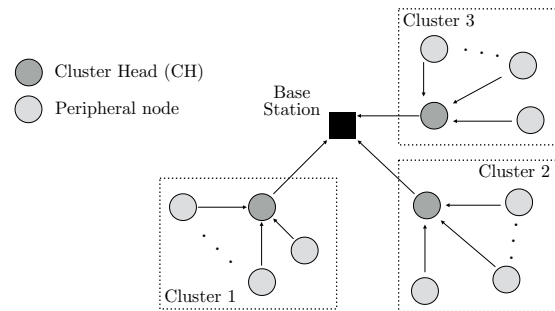

Fig. 1. The considered cluster-based network architecture.

is presented in Section III, whereas Section IV presents the proposed Copula-function-based correlation model in comparison to the conventional multivariate Gaussian model. Details on the derivation of the model parameters and encoding rates are given in Section V. Finally, experimental results are presented in Section VI, while Section VII concludes the work.

II. NETWORK MODEL AND BACKGROUND

A. Network Model

The WSN is organized into groups of neighboring sensor nodes called *clusters*. Each cluster comprises of an elected coordinator called *cluster head* (CH) and the *peripheral nodes* (see Fig. 1). Peripheral nodes measure temperature data, apply compression and error protection mechanisms and transmit the resulting data packets to the base station via their corresponding CH. The latter are group coordinators that organize data transfer, sleeping periods and data aggregation within each group, as well as convey the encoded data to the base station. In addition, each CH measures and transmits its own temperature data.

Each peripheral node has the processing capacity needed to become a CH. To prevent CH battery depletion, the CH changes periodically based on energy criteria [30], [31]. When the residual energy of the CH turns low, another CH is elected among the peripheral nodes. In this way, energy consumption is balanced within the cluster and the network lifetime increases [30], [31]. The cluster formation abides by well-known cluster-tree solutions for IEEE 802.15.4-based MAC protocols in WSNs, e.g., the IEEE 802.15.4 GTS [32].

B. Background on Slepian-Wolf Coding

Let (X_1, X_2) be two correlated *i.i.d.* (independent and identically distributed) temperature data sources obtained by two sensor nodes in a cluster. According to traditional source coding theory, in the lossless compression scenario, each sensor can encode its data independently at a rate greater or equal to the entropy, i.e., $R_{X_1} \geq H(X_1)$ and $R_{X_2} \geq H(X_2)$. If communication between the sensors is enabled, then the lowest total achievable encoding rate corresponds to the joint entropy, that is, $R_{X_1} + R_{X_2} \geq H(X_1, X_2)$. This can be achieved, for example, by encoding one source, say X_1, to its entropy $H(X_1)$, and the other source to its conditional entropy $H(X_2|X_1)$—by applying prediction and entropy coding. The
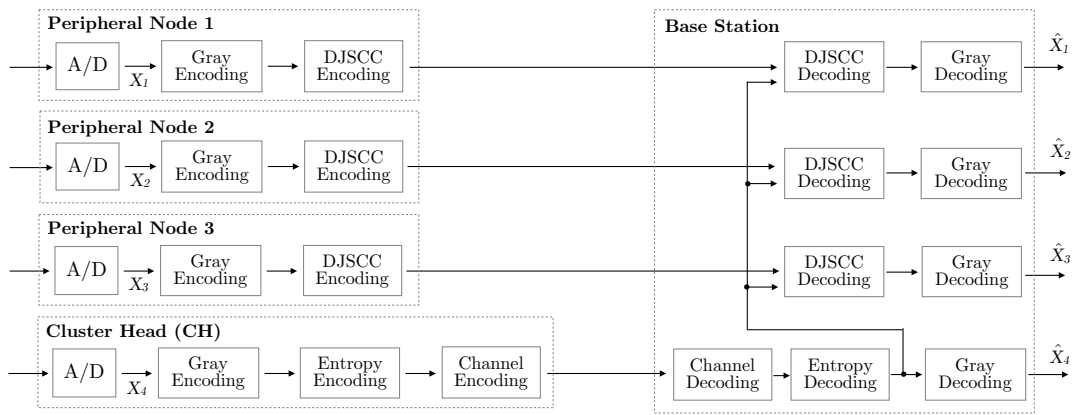
Fig. 2. The proposed system architecture.

Slepian-Wolf (SW) theorem [3] states that, if X_1 and X_2 are separately encoded and jointly decoded, the achievable rate region is still given by $R_{X_1} \geq H(X_1|X_2)$, $R_{X_2} \geq H(X_2|X_1)$, and $R_{X_1} + R_{X_2} \geq H(X_1, X_2)$. In the *asymmetric* SW coding scenario, one source is entropy encoded (at a rate $R_{X_2} \geq H(X_2)$) and used at the decoder as side information to decode the other source. The latter is SW encoded at a rate $R_{X_1} \geq H(X_1|X_2)$. In *non-asymmetric* SW coding, both sources (rather than one) are SW encoded and jointly decoded. In [6], Cover extended the SW theorem to the case of lossless MT coding of an arbitrary number of correlated, discrete, i.i.d. sources $X_1, X_2, ..., X_N$.

III. PROPOSED DISTRIBUTED JOINT SOURCE-CHANNEL CODING ARCHITECTURE

A. Overview

In the proposed architecture[1], shown in Fig. 2, the correlation between the data collected from the sensors within each cluster is exploited by means of SW coding. Particularly, let N be the total number of sensor nodes within a cluster, with the N-th node denoting the CH. According to the proposed coding scheme, the CH encodes its collected information, denoted by X_N, at a rate $R_{X_N} \geq H(X_N)$. Each of the $N - 1$ peripheral nodes within the cluster encodes the gathered data (denoted as $X_1, ..., X_{N-1}$, respectively) using asymmetric SW coding. That is, the corresponding encoding rates are $R_{X_n} \geq H(X_n|X_N), \forall n = 1, 2, ..., N - 1$. Since the information is transmitted over wireless links, channel encoding is required. Transmission is performed over the 16 channels of the IEEE 802.15.4 PHY and inter-sensor interference is mitigated via the utilized MAC layer cluster-tree coordination [32]. Conventional error protection, by means of channel encoding, is performed for the encoded data of the CH (see Fig. 2), while the proposed DJSCC is performed at the peripheral nodes. Assuming a statistical model for the cluster-level temperature data correlation, the base station decodes the information from the peripheral nodes using the decoded temperature data collected from the CH as side information (see Fig. 2).

[1] Without loss of generality, in the rest of the paper, our practical examples and illustrations consider a WSN where each cluster is formed by 4 nodes.

In the proposed system, we follow a SW rather than an MT code design for the following reason: As mentioned in Section II-A, the sensors in each cluster periodically elect a different CH so as to even out the energy consumption in the cluster. Under this requirement, MT source coding becomes difficult to deploy because, if one node does not send data, the decoding of the other nodes fails and the base station needs to reconfigure the entire encoding design. On the contrary, using a SW code design (in which the CH provides the side information), the encoding of the other nodes is not affected if a peripheral node fails (e.g., runs out of energy resources).

B. Practical Code Design

1) Source-Channel Coding of CH Information: Each sensor acquires discrete temperature samples through an analog-to-digital converter with b bit-depth accuracy. Under the memory capabilities of the sensor, m samples are aggregated together for encoding. Binarization is performed by means of gray encoding [33], resulting in an array of $k = m \times b$ bits to be encoded. Using gray encoding, the binary representations of two consecutive values differ in one bit position. This approach improves the performance of SW decoding, where the decoded CH information is used as side information. The binarized data is compressed using arithmetic entropy coding, achieving a source coding rate of $R_{X_N} \geq H(X_N)$ bits. The compressed bit-stream is then channel encoded resulting in the total transmitted information of $R'_{X_N} \geq \frac{H(X_N)}{C}$ bits, where C denotes the channel capacity. Channel encoding is realized using a Raptor code that adheres to the systematic design described in the Raptor RFC5053 standard [34]. At the decoder, the encoding operations are reversed resulting in the decoded signal.

2) Distributed Joint Source-Channel Code Design: Let $\mathbf{x}_n = [x_n^1(1), ..., x_n^1(b), ..., x_n^m(1), ..., x_n^m(b)]$ be $k = m \times b$ information bits, resulting after binarization and gray encoding (with b bits) of m digital samples from source X_n (i.e., the data source of a peripheral node $n = 1, 2, ..., N - 1$). Distributed joint source-channel encoding is applied to $\mathbf{x}_n$, realized by a SW Raptor encoder. Raptor codes are formed as a concatenation of a conventional precoding step and a Luby Transform (LT) [35] step. The precoding step comprises

an LDPC code that is used to *(i)* relax the condition on the number of edges of the LT and *(ii)* recover from decoding errors after the LT decoding stage. The LT codes provide the variable rate property and help to recover a constant fraction of the source symbols. Our SW design is also based on the Raptor RFC5053 standard [34], which defines a code distribution $\Omega(x)$, leading to stable and efficient code constructions. Moreover, the standard provides a fixed distribution, such that each output symbol corresponds to only one combination of input symbols. Thus, it is sufficient to know the output symbol index to determine the distribution of the input, thereby eliminating the need to send extra information to the decoder [28], [34].

Based on the Raptor RFC5053 standard [34], which defines a systematic code, we design a non-systematic[2] SW code construction that abides by the parity-based SW coding approach [2]. In order to maintain a simple SW encoder with reduced processing cost, our design does not include the Hamming precode step [34].

The Tanner graph of the designed non-systematic SW Raptor code in depicted in Fig. 3. At the encoder, the LDPC codeword is first formed as $\mathbf{y}^T = \mathbf{G}_{\text{LDPC}w \times k} \times \mathbf{x}^T$, where $w = k + s$ and $\mathbf{G}_{\text{LDPC}w \times k}$ is the generator matrix of the LDPC precode[3]. Then, the Raptor codeword is given by $\mathbf{c}^T = \mathbf{G}_{\text{LT}p \times w} \times \mathbf{y}^T$, where $\text{G}_{\text{LT}p \times w}$ is the generator matrix of the LT code. The $R_{X_n} = p$ bits from the output of the non-systematic Raptor encoder are transmitted. When noiseless transmission is considered then, for decoding with low error probability, we need that $R_{X_n} = p \geq kH(X_n|X_N)$ bits. The conditional entropy $H(X_n|X_N)$ depends on the correlation between the sources and its calculation is described in Section V. For transmission over a noisy channel, the transmission rate needs to be increased according to the channel capacity as $R_{X_n} = p \geq \frac{kH(X_n|X_N)}{C}$.

At the decoder, the information is obtained by applying soft-decoding by means of belief propagation [36] on the Raptor Tanner graph (see Fig. 3). To initiate decoding, the decoder is given the following soft-information in the form of log-likelihood ratios (LLRs): In the noiseless transmission case, the LLRs $L[x_n^*(i)]$, $i = 1, 2, \ldots p$, which correspond to the parity symbols for the encoded source X_n, are set to a very large positive or negative value (depending of the value of the received symbol). When transmission is performed over a binary additive white Gaussian noise (AWGN) channel and binary phase-shift keying (BPSK) modulation is considered[4], the LLR of each parity symbol is initialized as [37]

$$L[x_n^*(i)] = \frac{2}{\sigma_n^2} y_n(i), \tag{1}$$

where $y_n(i)$ is the value received when $x_n^*(i)$ is sent, and σ_n^2

[2]Apart from the non-systematic version of the code, we have also designed and tested a systematic Raptor SW code following the construction in [11]. We observed that the non-systematic code achieves better compression performance in short codelengths (smaller than 1000 bits), while the systematic code performs better for large codelengths. Since the monitored physical parameter (temperature) results in small codelengths we adhere to the non-systematic Raptor code construction.

[3]The LDPC code has a rate $\frac{k}{k+s}$, where s is the number of parity bits.

[4]The IEEE 802.15.4 standard considers BPSK modulation in the 868 and 915 MHz bands, and offset quadrature phase-shift keying (OQPSK) modulation in the 2.4 GHz band.
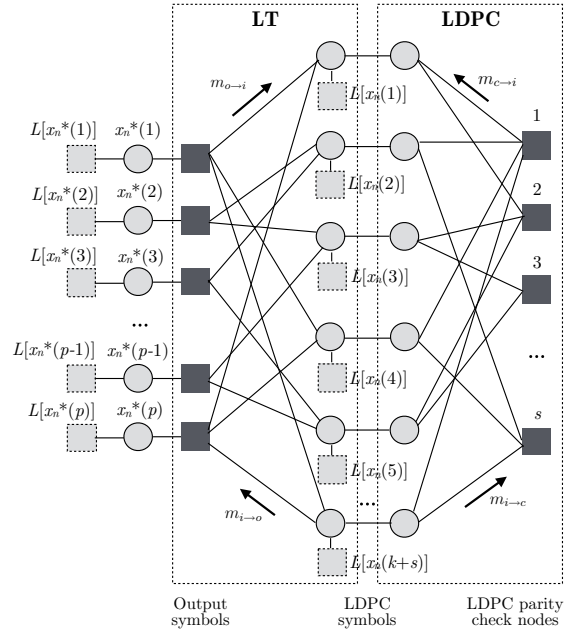

Fig. 3. Tanner graph of our non-systematic SW Raptor code. For simplicity, the index ℓ has been dropped from the notation for the LLR of each information symbol. The information symbol LLR is now denoted as $L[x_n(i)]$ with $i = 1, 2, ..., k$, where $k = m \times b$.

is the variance of the Gaussian noise. For transmission over a channel experiencing Rayleigh fading—assuming that the channel state information (CSI) is known at the decoder—the LLRs are given by [38]

$$L[x_n^*(i)] = \frac{2}{\sigma_n^2} y_n(i) \times r, \tag{2}$$

where r is the fading gain. These channel models are known to characterize the behavior of narrow-band transmission within personal area networks [39]. The LLR for each information binary symbol, $x_n^\ell(i)$ in $\mathbf{x}_n$, where $i = 1, 2, \ldots, b$ iterates over the bits of the binary representation of the sample $\ell = 1, 2, \ldots, m$, is initialized as

$$L[x_n^\ell(i)] = \log \frac{\Pr[x_n^\ell(i) = 0|x_N^\ell]}{\Pr[x_n^\ell(i) = 1|x_N^\ell]}$$
$$= \log \frac{\int_{x_n^\ell(i)=0} f(x_n|X_N = x_N^\ell)dx_n}{\int_{x_n^\ell(i)=1} f(x_n|X_N = x_N^\ell)dx_n}. \tag{3}$$

where x_N^ℓ denotes the ℓ-th sample from the CH data m-tuple, which acts as side information. The numerator of (3) is the integral of the conditional pdf of the correlation model (see Section IV) on the intervals where $x_n^\ell(i) = 0$, and the denominator is the integral of the pdf on the intervals where $x_n^\ell(i) = 1$ (see Section V).

The LLRs $L[x_n(i)], i = k + 1, ..., k + s$, which correspond to the parity symbols of the LDPC code, are initialized to zero as these symbols are not known *a priori* at the decoder.

Finally, after Raptor decoding is completed, the soft-information is converted to binary symbols via thresholding, and gray decoding is performed to obtain the decoded data.

IV. CORRELATION MODELING

We now focus on the modeling of the correlation between the temperature data sources captured by the sensor nodes. We first review the typical approach followed in the literature and then present the proposed copula-function-based model.

A. Multivariate Gaussian Correlation Model

A representative model for describing the correlation of information sources collected by WSN nodes is the multivariate Gaussian (MG) distribution [13], [18], [19], [21]. In the N-dimensional space consisting of the N nodes of the cluster, the joint probability density (pdf) function of the N random variables can be expressed by a multivariate normal distribution

$$f(x_1, x_2, ..., x_N) = \frac{1}{(2\pi)^{\frac{N}{2}} |\boldsymbol{\Sigma}|^{\frac{1}{2}}} \times \exp\left(-\frac{1}{2}(\mathbf{x} - \boldsymbol{\mu})^T \boldsymbol{\Sigma}^{-1}(\mathbf{x} - \boldsymbol{\mu})\right), \quad (4)$$

where $\mathbf{X} = (X_1, X_2, ..., X_N)$ is an N-dimensional vector consisting of the correlated random variables, $\boldsymbol{\mu} = (\mathrm{E}[X_1], \mathrm{E}[X_2], ..., \mathrm{E}[X_N])$ is the N-dimensional vector containing the mean values of the random variables and $\boldsymbol{\Sigma}$ is the covariance matrix of size $N \times N$.

The statistical dependencies of the measured data from the N nodes within a cluster are incorporated in the covariance matrix. The elements outside the main diagonal can be expressed using the Pearson correlation coefficient

$$\rho_{lj}^{(p)} = \frac{\mathrm{Cov}(X_l, X_j)}{\sqrt{(\mathrm{Var}(X_l)\mathrm{Var}(X_j))}}, \quad (5)$$

where the terms $\mathrm{Var}(X_l)$ and $\mathrm{Var}(X_j)$ represent the variances of the random variables X_l and X_j, respectively, with $l, j \in \{1, 2, ... N\}$.

Despite being typically used in the literature [13], [18], [19], [21], the MG model of (4) considers that the marginal distributions of the sensors are also Gaussian. This assumption is not always valid. For instance, the marginal statistics of temperature data gathered by a sensor from our deployment are depicted in Fig. 4. The figure shows that the marginal statistics cannot be accurately modeled with a Gaussian distribution. Beyond this aspect, it is worth noting that the Pearson correlation coefficient in (5) captures linear dependencies between random variables under the assumption of a Gaussian distribution of the data.

B. Proposed Copula-Function-Based Correlation Model

We propose the use of a Copula function (CF) [40] for a more generic and accurate modeling of data dependencies between the cluster nodes. As opposed to the MG model, when using a CF-based model, the correlation modeling approach is based on the actual marginal statistics of the random variables. In this way, the statistical properties of the temperature readings of each sensor are represented more accurately and, in turn, a more precise correlation model is derived.
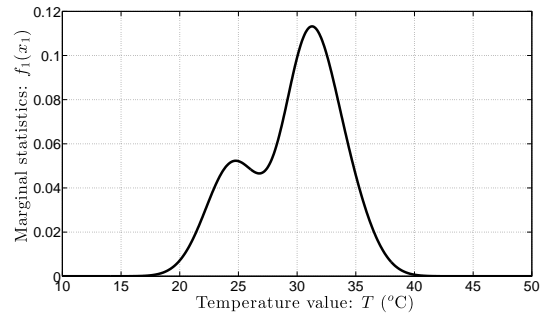

Fig. 4. Example of the marginal statistics of a peripheral node measuring temperature.

Let $\mathbf{X} = (X_1, X_2, ..., X_N)$ be the vector of the correlated random variables and let $F_1(X_1), F_2(X_2), ..., F_N(X_N)$ be their continuous marginal cumulative density functions (cdfs). Using the probability integral transform [41] on each X_n, $n = 1, 2, ... N$, a vector of random variables $(U_1, U_2, ..., U_N) = (F_1(X_1), F_2(X_2), ..., F_N(X_N))$ is created, where the components U_n are uniformly distributed. Therefore, regardless of the initial distribution of each random variable X_n, the transformed variable U_n always follows a uniform distribution. According to the Sklar's theorem [40], if F is the N-dimensional joint cdf of $\mathbf{X}$, there exists a unique N-dimensional copula function $C : [0,1]^N \to [0,1]$ such that for all $\mathbf{x} \in R^N$,

$$F(x_1, x_2, ..., x_N) = C(F_1(x_1), F_2(x_2), ..., F_N(x_N)). \quad (6)$$

Since a CF is a multivariate distribution function of uniform random variables, the following properties are valid: *(i)* $C(\mathbf{u}) = 0$, if at least one element of $\mathbf{u} = (u_1, u_2, ..., u_N)$, $\mathbf{u} \in [0,1]^N$, is zero (*grounded* property of a copula), *(ii)* $C(\mathbf{u}) = u_n$ if all elements of $\mathbf{u}$ are 1 except u_n, and *(iii)* C is N-increasing[5].

Differentiating (6) with respect to $u_1 = F_1(x_1), u_2 = F_2(x_2), ..., u_N = F_N(x_N)$, yields the joint pdf

$$f(x_1, x_2, ..., x_N) = c\left(F_1(x_1), F_2(x_2), ..., F_N(x_N)\right) \times f_1(x_1) \times f_2(x_2) \times ... \times f_N(x_N), \quad (7)$$

where $c\left(F_1(x_1), F_2(x_2), ..., F_N(x_N)\right)$ is the *copula density*. Equation (7) shows how the copula density controls the level of dependence between the random variables $X_n, n = 1, 2, ..., N$. For example, if $c(u_1, u_2, ..., u_N) = 1$, the joint pdf is the product of the marginal pdfs, that is, $X_1, X_2, ..., X_N$ are independent. Importantly, the CF model applies no restriction on the underlying marginal statistics, which may follow any probability distribution.

Given the marginal pdfs of the random variables, an appropriate copula that best captures the dependencies among the data should be selected. Several copula families have been proposed [23], [40], [42], with the elliptical form being the most common due to the ease in estimation for $N > 2$. The simplest elliptical CF is the Gaussian, which has the following

---

[5]This means that the CF volume of any N-dimensional interval is non-negative.

form [24], [40]:

$$C_G(\mathbf{u}) = \Phi_\Gamma(\Phi^{-1}(u_1), \Phi^{-1}(u_2), ..., \Phi^{-1}(u_N)), \quad (8)$$

where $u_n = F_n(x_n), n = 1, 2, ..., N$, Φ_Γ denotes the standard multivariate normal cdf with linear correlation matrix Γ, Φ denotes the standard univariate normal cdf, and Φ^{-1} denotes the inverse (quantile) function of Φ. Then, using Eq. (7) the multivariate distribution is expressed in terms of the Gaussian copula density function [43] as

$$f(x_1, x_2, .., x_N) = \frac{1}{|\Gamma|^{\frac{1}{2}}} \exp\left[-\frac{1}{2}\mathbf{v}\left(\Gamma^{-1} - \mathbf{I}\right)\mathbf{v}^{\mathrm{T}}\right] \prod_{n=1}^{N} f_n(x_n), \quad (9)$$

where $\mathbf{v} = [\Phi^{-1}(F_1(x_1)), \Phi^{-1}(F_2(x_2))..., \Phi^{-1}(F_N(x_N))]$ and $\mathbf{I}$ is the $N \times N$ identity matrix. To capture the dependence between the sensors' readings, a proper measure should be considered. When applying the CF-based model, the Pearson coefficient is not an appropriate measure, since the correlation among uniformly distributed random variables needs to be expressed. For that reason, we use the Spearman correlation coefficient, which is given by

$$\rho_{lj}^{(s)} = \frac{\mathrm{Cov}(U_l, U_j)}{\sqrt{(\mathrm{Var}(U_l)\mathrm{Var}(U_j))}}. \quad (10)$$

The Spearman coefficient is calculated empirically by estimating the empirical Pearson coefficient between the ranks of the data gathered by the sensors, as explained in Section V-B.

V. DETERMINATION OF THE MODEL PARAMETERS AND ENCODING RATES

In this section, we describe the derivation of the parameters and encoding rates for the conventional MG and the proposed CF-based correlation model.

A. MG Correlation Model

In the proposed system, described in Section III, we estimate the parameters of the MG model in each cluster based on offline training. Specifically, during the training stage, we collect measurements from the sensors in the cluster and derive the parameters of the covariance matrix Σ and the mean value vector $\boldsymbol{\mu}$. These parameters are then used to calculate the encoding rates and derive the soft-information for decoding based on belief propagation, as detailed in Section V-C. During the operation of the proposed system, the base station, which collects the data, can periodically refine the estimation of the modeling parameters.

B. Proposed CF-based Correlation Model

To apply the proposed CF-based model, the marginal pdfs $f_n(x_n)$, $n = 1, 2, ..., N$, and the correlation matrix Γ of the Gaussian copula need to be estimated. During an offline training stage, samples from several sensors were collected and the continuous marginal pdfs were estimated using the *kernel density estimation* (KDE) approach [44]:

$$f_n(x_n) = \frac{1}{M \times h_n} \sum_{i=1}^{M} K\left(\frac{x - x_i}{h_n}\right), \quad (11)$$

where M is the number of samples. The Gaussian kernel $K(v) = \frac{1}{\sqrt{2\pi}} \exp\left(-\frac{1}{2}v^2\right)$ for curve estimation was used due to its simplicity and good fitting accuracy. In addition, an appropriate smoothing parameter h_n was selected for each pdf $f_n(x_n)$ corresponding to each sensor $n = 1, 2, ..., N$.

The correlation matrix Γ has non-diagonal elements equal to the estimated Spearman's rho values and diagonal elements equal to 1. The Spearman coefficient is empirically estimated using training data collected from the sensors in each cluster. Specifically, starting from the original training data set $\{X_l(z), X_j(z)\}$, $z = 1, 2, ..., Z$—where Z denotes the size of the training data set—we estimate the set $\{\hat{U}_l(z), \hat{U}_j(z)\}$ as $\hat{U}_l(z) = \frac{1}{Z}\mathrm{rank}[X_l(z)]$ and $\hat{U}_j(z) = \frac{1}{Z}\mathrm{rank}[X_j(z)]$, where $\mathrm{rank}[X_l(z)]$ denotes the rank of $X_l(z)$. Hence, the estimated values $\{\hat{U}_l(z), \hat{U}_j(z)\}$ are the standardized ranks, which are good approximations for the pairs $\{U_l(z), U_j(z)\} = \{F_l(X_l(z)), F_j(X_j(z))\}$. The Spearman coefficient can then be calculated using (10).

C. Encoding Rates

In the architecture of Fig. 2, in order to derive the LLRs and the encoding rate for each peripheral node, we need to estimate the conditional statistics $f(x_n|x_N)$ and the conditional entropy $H(X_n|X_N)$. To this end, based on the multivariate models defined by (4) and (9), we first derive the univariate distribution, $f_N(x_N)$, for the marginal statistics of the CH node, and the bivariate distribution, $f(x_n, x_N), \forall n \in \{1, 2, ..., N-1\}$. That is,

$$f_N(x_N) = \int_{X_1} ... \int_{X_{N-1}} f(x_1, ..., x_N)dx_1...dx_{N-1}, \quad (12)$$

and

$$f(x_n, x_N) = \int_{X_{l\neq\{n,N\}}} ... \int_{X_{j\neq\{n,N\}}} f(x_l, ..., x_j) \\ \times dx_{l\neq\{n,N\}}...dx_{j\neq\{n,N\}}, \quad (13)$$

where $f(x_1, x_2, ..., x_N)$ is either the MG or the CF-based pdf defined in (4) and (9), respectively. Given the joint and marginal pdfs, the conditional pdf is derived as

$$f(x_n|x_N) = \frac{f(x_n, x_N)}{f_N(x_N)}. \quad (14)$$

The conditional pdf for each model is used in the calculation of the LLRs in (3). It is important to note that adhering to this modeling approach, namely, deriving the bivariate distribution from the estimated multivariate distribution instead of directly estimating the bivariate model, allows for arbitrary changing the CH node (see the network model description in Section II-A) without requiring to recompute the model parameters Σ and Γ.

To derive the encoding rate per peripheral sensor $n = 1, 2, ..., N-1$, we proceed as follows: Since the A/D converter of each sensor provides a discrete version of a sensed continuous value, the continuous pdf is transformed into a probability mass function (pmf). To this end, the range of each continuous random variable X_n is divided into intervals

of length Δ, specified by the A/D resolution. As the A/D resolution is high[6], we can approximate the marginal pmf as

$$p(x_{n(\tau)}) = \int_{\tau\Delta}^{(\tau+1)\Delta} f_n(x_n)dx_n \approx f_n\left(\frac{(2\tau+1)\Delta}{2}\right)\Delta, \tag{15}$$

where $p(x_{n(\tau)})$ is the probability that the continuous parameter takes value in the τ-th interval and $n = 1, 2, ..., N$. Similarly, for the joint pmf, we have

$$p(x_{n(\tau)}, x_{N(\theta)}) = \int_{\tau\Delta}^{(\tau+1)\Delta} \int_{\theta\Delta}^{(\theta+1)\Delta} f(x_n, x_N)dx_n dx_N$$
$$= f\left(\frac{(2\tau+1)\Delta}{2}, \frac{(2\theta+1)\Delta}{2}\right)\Delta^2. \tag{16}$$

Using the marginal and joint pmfs in (15) and (16), we calculate the entropy $H(X_N)$ and the joint entropy $H(X_n, X_N)$. Then, the conditional entropy for each source X_n given X_N is computed as

$$H(X_n|X_N) = H(X_n, X_N) - H(X_N), \forall n \in \{1, ..., N-1\}. \tag{17}$$

The conditional entropy in (17) is expressed in bits per temperature sample. To express the encoding rate per peripheral node $n = 1, 2, ..., N-1$ in bits per binary symbol, as required by our analysis in Section III, we divide the conditional entropy $H(X_n|X_N)$ by the bit-depth b of the A/D converter.

VI. EXPERIMENTAL EVALUATION

For the experimental evaluation of the proposed work, we deployed a WSN comprising 16 nodes gathering temperature data. Our deployment took place within an indoor office environment, where sensors were mounted to walls with an average distance of 6 meters[7] and a temperature variation of up to $20°C$ was observed within a 24-hour cycle. The utilized hardware for the sensors and the base station (sink node) is described in Table I.

The network architecture was aligned with the description in Section II-A. Within each cluster, the number of sensor nodes was $N = 4$ and they were chosen to be co-located; three of them being peripheral nodes and the fourth being the CH. The sink node was connected to a desktop computer where data collection and decoding took place. To ensure collision-free packet transmissions at the MAC layer, transmissions within each cluster occurred at different channels of the IEEE 802.15.4 PHY via the AT86RF230 transceiver. The IEEE 802.15.4 GTS [32] was used for the intra-cluster superframe beaconing and the scheduling of packet transmissions. The payload packet size was set to 80 bytes. All residual transmission impairments incurred from external sources (e.g., interference from co-located IEEE 802.15.4 or WiFi networks) were mitigated via the default PHY layer protection or the proposed DJSCC scheme.

The sensors operated at a sampling rate of 2Hz. We aggregated $m = 40$ consecutive measurements to construct a data-block of size $k = m \times b = 640$ bits, where $b = 16$

[6]In this work, A/D conversion was performed on 16 bits.

[7]This test was carried out within the auspices of a commercial service development from InterNET SRL, OFRIM Group Member.
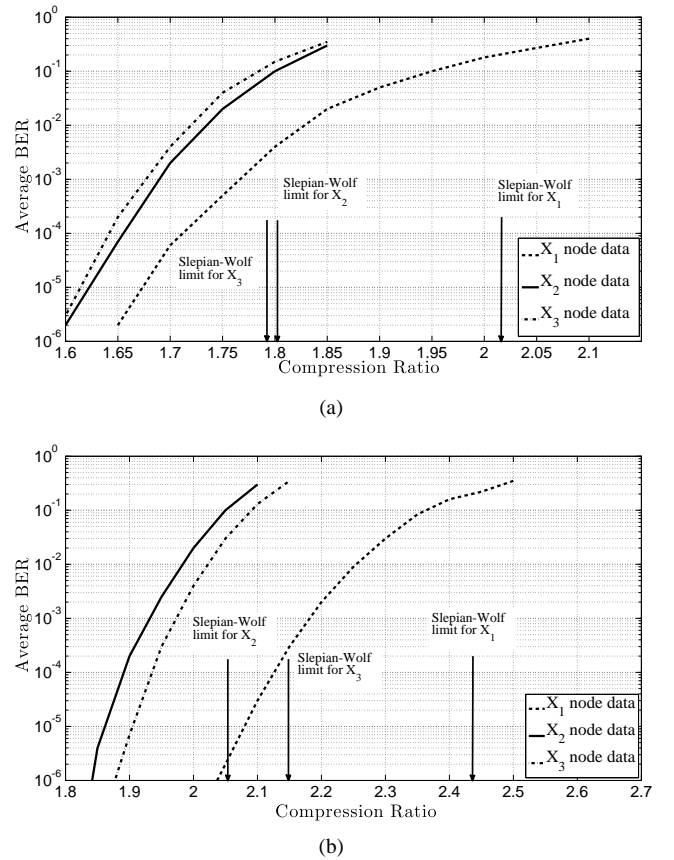

Fig. 5. Average BER of the decoded information vs. compression ratio, $\frac{1}{H(X_n|X_N)}$, for (a) the Multivariate Gaussian, and (b) the proposed Copula-function-based correlation model.

bits is the bit-depth of the A/D converter within each sensor. The size of the encoded data-block strikes a balance amongst good compression performance (where a long codeword is advantageous), low latency and memory requirements.

During the training stage, data collected over a three-day operation of the WSN were used to derive the parameters of the MG and the proposed CF-based model. In particular, as described in Section V, we computed the covariance matrix Σ and the mean-vector μ for the MG model while, for the proposed CF model, we calculated the correlation matrix Γ and we estimated the marginal pdfs $f_n(x_n)$ using (11). The encoding rates for each peripheral node were then estimated as described in Section V.

To evaluate the compression performance and the error-resilience capability of the proposed system we collected additional data (different from the training data) over a thirty-day operation period of the system.

A. Compression Performance Evaluation

Initially, we assess the compression capacity of the proposed Raptor-based SW code design. In particular, we evaluate the bit-error-rate (BER) of the decoded data from each peripheral sensor, $X_n, n = 1, 2, 3$, with respect to the compression ratio $\frac{1}{H(X_n|X_N)}$, where X_N denotes the data collected from the CH (i.e., the side information). Average results over 200 trials are

TABLE I
HARDWARE SPECIFICATION OF THE PERIPHERAL, CH AND SINK NODES

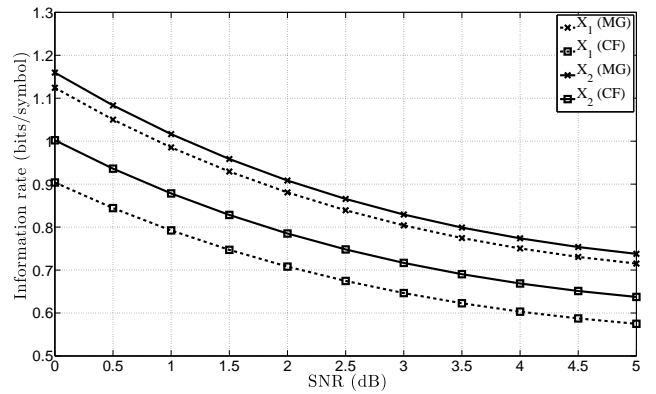| Peripheral or CH Node |
| --- |
| Microcontroller Atmel ATmega 1281 |
| Transmitter AT86RF230 |
| Dual-chip antenna |
| Microchip MCP9700AT Temperature Transducer (-40 to $+150°$C) |
| TAOS Luminosity Intensity Transducer TSL250R |
| Li-Polymer Battery - 3.7V |
| Battery Charger with USB port |
| Dimensions: 60mm x 33mm |
| **Base Station (Sink Node)** |
| Microcontroller Atmel ATmega 1281 |
| Transmitter AT86RF230 |
| Dual-chip antenna |
| USB-UART Bridge for connection to PC USB port |
| Dimensions: 48mm x 21mm |

TABLE II
COMPARISON OF AVERAGE ENCODING RATES (IN BITS/DATA-BLOCK)
FOR ENTROPY CODING, AND SLEPIAN-WOLF CODING WITH THE
EXISTING MULTIVARIATE AND THE PROPOSED
COPULA-FUNCTION-BASED CORRELATION MODEL (X_4 DENOTES THE
CH DATA THAT IS ALWAYS ENTROPY ENCODED).

	X_1	X_2	X_3	X_4
Entropy Coding	452	496	512	471
Proposed with MG	319	356	358	—
Gain w.r.t. Entropy Coding (%)	29.43	28.23	30.08	—
Proposed with CF	263	312	303	—
Gain w.r.t. Entropy Coding (%)	41.81	37.10	40.82	—
Gain w.r.t. MG Model (%)	17.56	12.36	15.36	—

Fig. 6. Information rate versus SNR for transmission of the readings from sensors X_1 and X_2 over (a) the AWGN channel and (b) the Rayleigh fading channel. The proposed DJSCC system uses either the conventional MG or the proposed CF-based correlation model.
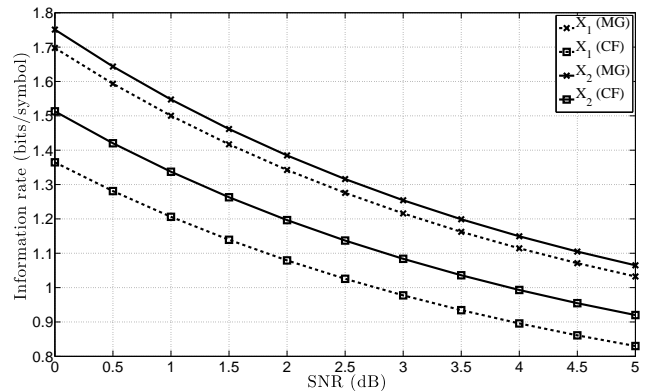
presented. Per trial, a four-day period (out of the full thirty-day period) was selected at random and the corresponding temperature data was compressed. The average compression performance obtained with the proposed CF-based correlation model is compared against the average performance achieved with the conventional MG model, which is considered in state-of-the-art works—see, for example, [13], [18], [19]. The results, together with the theoretical SW limits, are presented in Fig. 5(a) and Fig. 5(b) for the MG and the proposed CF-based correlation model, respectively. With respect to the reconstruction quality of the decoded temperature data, BER values below 10^{-6} corresponded to near-lossless recovery. On the other end, values around 10^{-2} lead to maximum root mean squared-error of 128, which corresponds to a temperature error of up to $0.38°$C, which is below the A/D accuracy of the utilized temperature transducer.

Contrasting the results in Figs. 5(a) and (b), we notice that, for the same average BER, the proposed system systematically achieves a higher compression ratio when the data correlation is expressed by the proposed CF-based correlation model. Moreover, when using the proposed model, our practical code design approximates the theoretical SW limit closer than when employing the conventional MG model. The results demonstrate that the proposed CF-based model expresses the correlation between the data captured by the different sensors with a higher accuracy than the conventional MG model.

Next, we compare the compression performance of the proposed system against the performance obtained with the baseline system, which performs arithmetic entropy coding of each sensor's readings. In both cases, lossless encoding is achieved, that is, the decoded temperature values of each node match the corresponding measured values. The average encoding rates (in bits per encoded data-block) achieved with the baseline system and the proposed system are reported in Table II. The results show that, when using the conventional MG correlation model, the proposed system reduces the required rate for compression by up to 30.08% compared to the baseline system. When the proposed CF-based model is used, the obtained improvements in rate reduction over the baseline system can reach up to 41.81%. We observe that using the proposed CF-based model reduces the encoding rate by up to 17.56% compared to using the conventional MG model. These gains highlight the importance of properly leveraging the correlation between the data gathered by the sensors in the WSN.

B. Joint Source-Channel Coding Performance Evaluation

We now evaluate the joint source-channel coding performance of the proposed system. Interference and packet losses cannot be controlled in our practical deployment, as such conditions vary during the operational lifetime of our system due to various external factors. For this reason, we have carried

out our evaluation using the AWGN and Rayleigh fading channel models under varying signal-to-noise-ratio (SNR) values. These models are well-known to provide for a good characterization of the behavior of narrow-band transmission within personal area networks [39]. Moreover, by using them we enable a reproducible experiment for both correlation models, and enable their comparison under the same communication channel conditions. We note that no retransmission of erroneous packets is required when using the proposed DJSCC system, as channel impairments are mitigated with the Raptor code present in the proposed design (see Section III-B2)

To carry out our evaluation, we derive the required information rate to achieve a decoding BER close to zero (BER $< 10^{-6}$) for different channel SNRs. The DJSCC performance of the system using the proposed CF-based correlation model is compared against the performance obtained with the conventional MG model. The results for temperature sensors X_1 and X_2, and for both communication channel models are depicted in Fig. 6. As expected, the required information rates for near-error-free decoding decrease with the SNR value. Moreover, for the same SNR, Rayleigh fading noise requires more rate to cope with than AWGN. Importantly, the results demonstrate the superior performance of our system when the proposed CF-based correlation model is used to express the correlation amongst the data gathered by the sensors. The significant improvements (up to 19.64% in information rate reduction) offered by the proposed correlation model over the conventional MG model are systematic over the different SNR conditions, sources (X_1 and X_2) and channel models.

C. Energy Savings

Under the channel conditions described in Section VI-B, we evaluate the energy consumption of a sensor running the proposed versus the baseline system. Specifically, each sensor in our WSN deployment runs executable programs implementing the proposed DJSCC scheme using the MG and the CF-based correlation model, as well as the baseline system. The information rates for our system and the packet retransmission limit for the baseline system are preset via the channel-model-based measurements described in Section VI-B. Full packets (80 bytes payload and 12 bytes header) are transmitted by aggregating encoded information from consecutive codewords when required. The Atmel ATmega 1281 microcontroller of each sensor is set to report its battery level once per minute during the execution. By gathering the battery level measurements from all sensors at the end of the experiment and converting them to available energy levels, we determine the percentile energy consumption difference between the proposed DJSCC and the baseline system. It is worth noticing that this energy consumption difference includes both the computational and transmission parts of the system. Average results over multiple executions and all sensors within a cluster are reported in Fig. 7. Results for both channel models and different SNR conditions are provided.

We observe that the proposed DJSCC system with CF-based correlation modeling yields a significant reduction in energy consumption with respect to the baseline system.
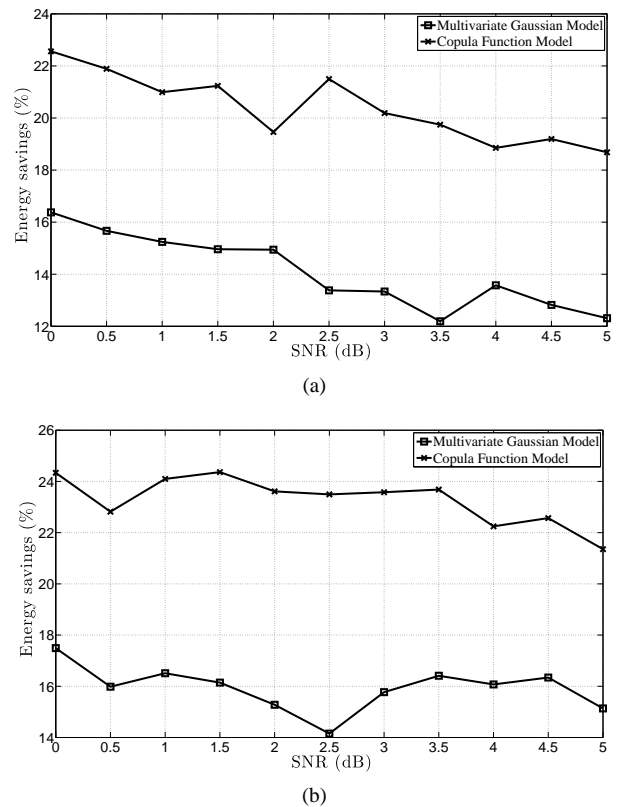

Fig. 7. Energy savings percentage vs SNR for the proposed DJSCC coding scheme using the MG or the proposed CF-based correlation model. Transmission is done over (a) AWGN channel, and (b) Rayleigh Fading channel.

When transmission faces AWGN, energy consumption savings between 18.68% to 22.56% are reported while, in the case of Rayleigh fading savings between 21.35% to 24.36% are observed. These savings are attributed to the following reasons: First, the proposed DJSCC scheme eliminates packet retransmissions due to the inherent error correcting capability of the code design. On the contrary, retransmissions are used to deal with channel impairments when the baseline system is used. Second, as shown in Section VI-A, the proposed system achieves higher compression rates than the baseline system as it exploits the correlation amongst the readings from different sensors.

We notice that, under both channel models, using the proposed CF-based correlation model systematically results in higher energy consumption reductions than using the conventional MG model. This is because, as shown in Section VI-B, using the proposed CF-based model our system achieves lower information rates for the same SNR conditions than using the conventional MG model.

VII. CONCLUSION

A novel DJSCC design for wireless sensors measuring temperature data has been presented. Our scheme is based on a new non-systematic SW Raptor code, which, unlike existing schemes (e.g., [11], [12]), achieves good performance for the short code lengths required by the application. A key contribution has been a novel Copula-function-based model

to express the inter-sensor data correlation. Experimentation using a WSN deployment shows that the proposed model significantly improves the compression performance of our system, by up to 17.56% in compression rate reduction, compared to the conventional multivariate Gaussian (MG) model, used in state-of-the-art works, e.g. [13], [19]. Moreover, under the same channel conditions, the proposed CF-based model is shown to yield a vast reduction (up to 19.64%) of the required transmission rate for error-free decoding compared to the MG model. By exploiting the inter-sensor data correlation at the decoder, the proposed DJSCC system achieves compression rate savings of up to 41.81% compared to the baseline system that performs arithmetic entropy encoding of the data. The high compression performance of our system in conjunction with its inherent error-resilience, which mitigates packet retransmissions, yield significant energy savings at the sensor (by up to 24.36%) with respect to the baseline system.

REFERENCES

[1] J. Yick, B. Mukherjee, and D. Ghosal, "Wireless sensor network survey," *Computer networks*, vol. 52, no. 12, pp. 2292–2330, 2008.

[2] Z. Xiong, A. D. Liveris, and S. Cheng, "Distributed source coding for sensor networks," *IEEE Signal Processing Magazine*, vol. 21, no. 5, pp. 80–94, 2004.

[3] D. Slepian and J. K. Wolf, "Noiseless coding of correlated information sources," *IEEE Transactions on Information Theory*, vol. 19, no. 4, pp. 471–480, Apr. 1973.

[4] A. D. Wyner and J. Ziv, "The rate-distortion function for source coding with side information at the decoder," *IEEE Transactions on Information Theory*, vol. 22, no. 1, pp. 1–10, Jan. 1976.

[5] T. Berger, "Multiterminal source coding," *The information theory approach to communications*, vol. 229, pp. 171–231, 1977.

[6] T. Cover, "A proof of the data compression theorem of Slepian and Wolf for ergodic sources," *IEEE Transactions on Information Theory*, vol. 21, no. 2, pp. 226–228, 1975.

[7] S. Pradhan and K. Ramchandran, "Distributed source coding using syndromes (DISCUS): Design and construction," *IEEE Transactions on Information Theory*, vol. 49, no. 3, pp. 626–643, Mar. 2003.

[8] V. Stankovic, A. D. Liveris, Z. Xiong, and C. N. Georghiades, "On code design for the Slepian—Wolf problem and lossless multiterminal networks," *IEEE Transactions on Information Theory*, vol. 52, no. 4, pp. 1495–1507, Jun. 2006.

[9] J. Garcia-Frias and Y. Zhao, "Compression of correlated binary sources using Turbo codes," *IEEE Commun. Lett.*, vol. 5, no. 10, pp. 417–419, Oct. 2001.

[10] A. Liveris, Z. Xiong, and C. Georghiades, "Compression of binary sources with side information at the decoder using LDPC codes," *IEEE Communications Letters*, vol. 6, no. 10, pp. 440–442, Oct. 2002.

[11] M. Fresia, L. Vandendorpe, and H. V. Poor, "Distributed source coding using raptor codes for hidden markov sources," *IEEE Transactions on Signal Processing*, vol. 57, no. 7, pp. 2868–2875, 2009.

[12] Q. Xu, V. Stankovic, and Z. Xiong, "Distributed joint source-channel coding of video using raptor codes," *IEEE Journal on Selected areas in communications*, vol. 25, no. 4, pp. 851–861, 2007.

[13] R. Cristescu, B. Beferull-Lozano, and M. Vetterli, "Networked slepian-wolf: theory, algorithms, and scaling laws," *IEEE Transactions on Information Theory*, vol. 51, no. 12, pp. 4057–4073, 2005.

[14] S. S. Pradhan, J. Kusuma, and K. Ramchandran, "Distributed compression in a dense microsensor network," *IEEE Signal Processing Magazine*, vol. 19, no. 2, pp. 51–60, Mar. 2002.

[15] F. Oldewurtel, M. Foks, and P. Mahonen, "On a practical distributed source coding scheme for wireless sensor networks," in *IEEE Vehicular Technology Conference, VTC Spring 2008*. IEEE, 2008, pp. 228–232.

[16] F. Oldewurtel, J. Ansari, and P. Mahonen, "Cross-layer design for distributed source coding in wireless sensor networks," in *Proc. International Conference on Sensor Technologies and Applications (SENSORCOMM)*. IEEE, 2008, pp. 435–443.

[17] F. Chen, M. Rutkowski, C. Fenner, R. Huck, S. Wang, and S. Cheng, "Compression of distributed correlated temperature data in sensor networks," in *Proc. Data Compression Conference (DCC)*, 2013, pp. 479–479.

[18] S. Cheng, "Multiterminal source coding for many sensors with entropy coding and Gaussian process regression," in *Proc. IEEE Data Compression Conference*. IEEE, 2013, pp. 480–480.

[19] Y. Yang, V. Stankovic, Z. Xiong, and W. Zhao, "On multiterminal source code design," *IEEE Transactions on Information Theory*, vol. 54, no. 5, pp. 2278–2302, 2008.

[20] J. E. Barceló-Lladó, A. M. Pérez, and G. Seco-Granados, "Enhanced correlation estimators for distributed source coding in large wireless sensor networks," *IEEE Sensors Journal*, vol. 12, no. 9, pp. 2799–2806, 2012.

[21] B. Beferull-Lozano and R. L. Konsbruck, "On source coding for distributed temperature sensing with shift-invariant geometries," *IEEE Transactions on Communications*, vol. 59, no. 4, pp. 1053–1065, 2011.

[22] P. K. Trivedi and D. M. Zimmer, *Copula modeling: an introduction for practitioners*. Now Pub, 2007, vol. 1.

[23] P. J. Danaher and M. S. Smith, "Modeling multivariate distributions using copulas: Applications in marketing," *Marketing Science*, vol. 30, no. 1, pp. 4–21, 2011.

[24] K. C. Barr and K. Asanović, "Energy-aware lossless data compression," *ACM Transactions on Computer Systems*, vol. 24, no. 3, pp. 250–291, 2006.

[25] D. I. Sacaleanu, R. Stoian, D. M. Ofrim, and N. Deligiannis, "Compression scheme for increasing the lifetime of wireless intelligent sensor networks," in *Proc. European Signal Processing Conference (EUSIPCO)*, 2012, pp. 709–713.

[26] F. Marcelloni and M. Vecchio, "A simple algorithm for data compression in wireless sensor networks," *IEEE Communications Letters*, vol. 12, no. 6, pp. 411–413, 2008.

[27] M. Vecchio, R. Giaffreda, and F. Marcelloni, "Adaptive lossless entropy compressors for tiny iot devices," *IEEE Transactions on Wireless Communications*, vol. 13, no. 2, pp. 1088–1100, 2014.

[28] A. Shokrollahi, "Raptor codes," *IEEE Transactions on Information Theory*, vol. 52, no. 6, pp. 2551–2567, 2006.

[29] T. Mladenov, S. Nooshabadi, and K. Kim, "Implementation and evaluation of raptor codes on embedded systems," *IEEE Transactions on Computers*, vol. 60, no. 12, pp. 1678–1691, 2011.

[30] K. Akkaya and M. Younis, "A survey on routing protocols for wireless sensor networks," *Ad hoc networks*, vol. 3, no. 3, pp. 325–349, 2005.

[31] D. I. Săcăleanu, D. M. Ofrim, R. Stoian, and V. Lăzărescu, "Increasing lifetime in grid wireless sensor networks through routing algorithm and data aggregation techniques," *International Journal of Communications*, no. 4, pp. 157–164, 2011.

[32] A. Koubaa, M. Alves, M. Attia, and A. Van Nieuwenhuyse, "Collision-free beacon scheduling mechanisms for IEEE 802.15.4/Zigbee cluster-tree wireless sensor networks," in *Proc. of the 7th Int. Worksh. on Appl. and Serv. in Wireless Netw. (ASWN)*, 2007.

[33] F. Gray, "Pulse code communication," March 1953, US Patent 2,632,058.

[34] M. Luby, A. Shokrollahi, M. Watson, and T. Stockhammer, "Rate raptor forward error correction scheme for object delivery," *Patent Document, RFC5053*, 2007.

[35] M. Luby, "Lt-codes," in *43rd Symposium on Foundations of Computer Science (FOCS'02)*. IEEE Computer Society, November 2002.

[36] J. Pearl, *Probabilistic reasoning in intelligent systems: networks of plausible inference*. Morgan Kaufmann, 1988.

[37] S. J. Johnson, "Iterative error correction," *The Edinburgh Building, Cambridge CB2 8RU, UK, Cambridge*, 2010.

[38] J. Hou, P. H. Siegel, and L. B. Milstein, "Performance analysis and code optimization of low density parity-check codes on rayleigh fading channels," *IEEE Journal on Selected Areas in Communications*, vol. 19, no. 5, pp. 924–934, 2001.

[39] A. F. Molisch, K. Balakrishnan, C.-C. Chong, S. Emami, A. Fort, J. Karedal, J. Kunisch, H. Schantz, U. Schuster, and K. Siwiak, "Ieee 802.15. 4a channel model-final report," *IEEE P802*, vol. 15, no. 04, p. 0662, 2004.

[40] R. B. Nelsen, *An introduction to copulas*. Springer Verlag, 1999.

[41] C. Genest and L.-P. Rivest, "On the multivariate probability integral transformation," *Statistics & Probability Letters*, vol. 53, no. 4, pp. 391–399, 2001.

[42] H. Joe, *Multivariate models and multivariate dependence concepts*. CRC Press, 1997, vol. 73.

[43] R. T. Clemen and T. Reilly, "Correlations and copulas for decision and risk analysis," *Management Science*, vol. 45, no. 2, pp. 208–224, 1999.

[44] G. G. Roussas, *An introduction to probability and statistical inference*. Academic Press, 2003.